38th International Electric Vehicle Symposium and Exhibition (EVS38)
Göteborg, Sweden, June 15-18, 2025

Managing the Quantity of Battery Data Required to Deliver High Accuracy Ageing Models and Support the Battery Passport

Maite Etxandi-Santolaya[1], Tomas Montes[1,2], Josh Eichman[1]
[1]*Department of Energy Systems Analytics, Institut de Recerca en Energia de Catalunya – IREC*
Barcelona, Spain
Corresponding author: metxandi@irec.cat
[2]*Department of Engineering Projects and Construction, Universitat Politècnica de Catalunya – UPC*
Barcelona, Spain

Executive Summary

Today's world is marked by a significant increase in the amount of data generated, and Electric Vehicles batteries are no exception. Although the importance of analysing and storing battery data is clear, methods to characterize dynamic profiles, distinctive of real-driving, are not standardized. This study evaluates different ways of characterizing Electric Vehicle battery data, balancing data volume and battery health assessment accuracy. Different features are extracted and used to build degradation models. Voltage and State of Charge show the most relevance for degradation prediction and boxplot-based characterization yields the best model performance. Data aggregation, meaning storing only relevant features per driving cycle, is proposed as the best method to reduce data quantity and generate accurate results, especially when employing histogram-based models. The results of this study can be used to guide feature selection for degradation models, reduce the dimensionality of laboratory datasets and as information for the Battery Passport.

Keywords: Electric Vehicles, AI - Artificial intelligence for EVs, Batteries, Battery Management System, Sustainable Energy

1 Introduction

The Electric Vehicle (EV) is positioned to drive the global transition to sustainable transportation in the next years. Beyond reducing emissions, the broader shift towards circularity in the EV industry is gaining importance, with increasing focus on reselling EVs and repurposing their batteries for second-life applications [1]. An enabler of this circular approach is the Battery Passport, a digital record that tracks key information about a battery throughout its lifecycle, from manufacturing to End of Life (EoL). This comprehensive system includes detailed information on battery composition, carbon footprint, and performance history, ensuring compliance, transparency and traceability [2].

One important category of information in the Battery Passport is the battery's usage history, as it is key for determining which EoL treatment the battery should follow. The analysis of battery usage is essential for two key aspects. Firstly, variations in driving patterns, charging habits, and environmental conditions

lead to diverse degradation rates in the battery. These factors significantly impact the battery's State of Health (SoH) and its Remaining Useful Life (RUL). Both indicators are critical in deciding whether the EoL battery can be resold, repurposed, or directed to recycling [3]. However, recently there has been an increased focus on the State of Function (SoF), which represents how functional a battery is at a given state for a particular driver and allows to tailor EoL estimation for each case [4]. Historical usage data also encapsulates key information about driving patterns that define the requirements to be considered for the SoF.

Given the vast amount of data generated throughout a battery's life, there is a need to reduce data volume by extracting key features to capture essential information. The Battery Regulation Annex XIII provides a broad framework to characterize battery operation, requiring information on the number of charging and discharging cycles, negative events (e.g., accidents), and environmental operating conditions, like temperature and State of Charge (SoC). However, the exact technical features and metrics that should be included in the Battery Passport are not fully standardized and may leave room for interpretation.

In this sense, degradation models play a crucial role in establishing the relationship between operational stress factors during usage and the rate of degradation. Many existing models rely on static laboratory testing, where cycling conditions are controlled and simplified. In these scenarios, degradation is typically characterized using parameters such as the C-rate, temperature, Depth of Discharge (DoD), and average SoC [5, 6]. While this approach yields valuable insights, it falls short of capturing the dynamic nature of real-world EV driving conditions. In real-world applications, the C-rate, temperature, SoC and voltage are subject to constant fluctuations, rendering static models inadequate for accurately predicting battery health and lifespan. Considering just the average values from the battery operation curves may miss on important information.

The goal of this study is to address this limitation by analyzing dynamic EV battery operation data and evaluating different methods to characterize it. The goal is to identify the features that most accurately represent real-world conditions and drive the degradation of the battery as represented by the SoH. Besides the usage of the proposed methods for the Battery Passport and degradation models, by reducing the high-frequency time-series data to lower-dimensional key features, the study aims to streamline the representation of historical usage, making it suitable for storing extensive laboratory data efficiently.

2 Methodology

The methodology of this study is based on long-term ageing tests conducted on six battery cells over a period of two years, as described in Section 2.1. Various approaches to characterize the time-series recorded during driving are evaluated in Section 2.2 to identify the features that best represent battery ageing. Using these features, a baseline degradation model is developed as explained in Section 2.3. Subsequently, in Section 2.4 different data reduction techniques are explored to assess the trade-off between predictive accuracy and data storage requirements. A visual summary of the methodology is provided in Figure 1.

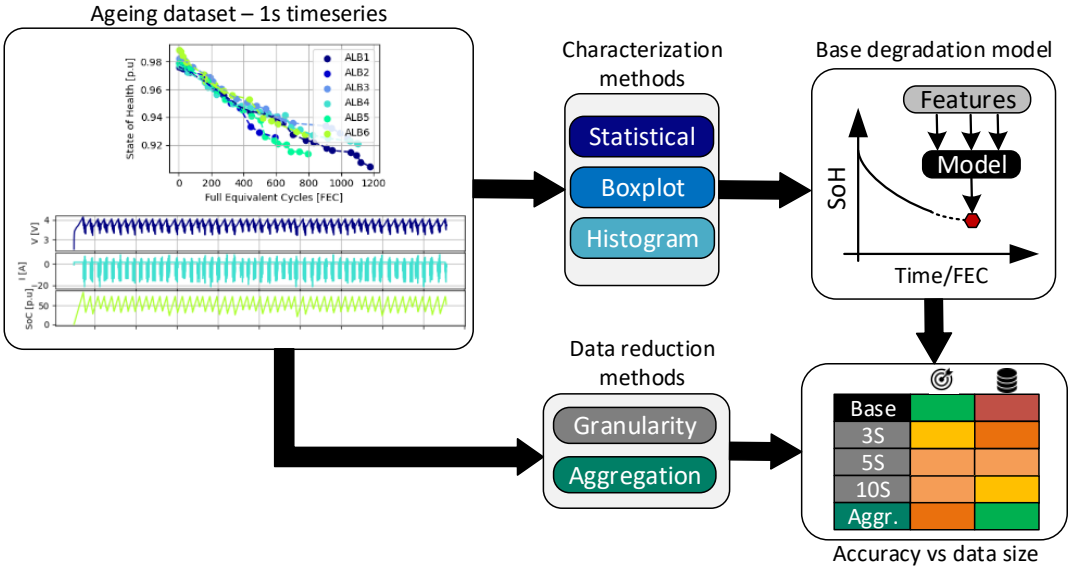

Figure 1: Graphical representation of the methodology of the study.

2.1 Data description

The data employed for this study contains the laboratory cycling of 6 cells labeled as ALB1-ALB6. The cell model is the one employed to build the battery packs for the EV in the H2020 Albatross project [7]. A summary of the cell characteristics is presented in Table 1.

Table 1: Characteristics of the cell tested in the laboratory

Manufacturer	LG Chem
Model	INR21700-M50T
Positive Electrode	LiNiMnCoO2
Negative electrode	graphite and silicon
Diameter	21.44 mm
Length	70.80 mm
Weight	69.25 g
Nominal Capacity (Q_{nom})	4.85 Ah
Nominal Voltage	3.63 V
Charge cutoff Voltage	4.2 V
Discharge cutoff Voltage	2.5 V
Cutoff current	50 mA

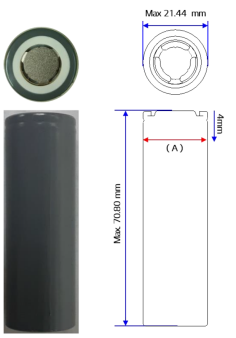

The testing protocol consists of repeated cycling for battery ageing and Reference Performance Test (RPT) for characterization. Figure 2 shows an example of a cycling test between two RPTs, with zoom-in views on each of the periods.

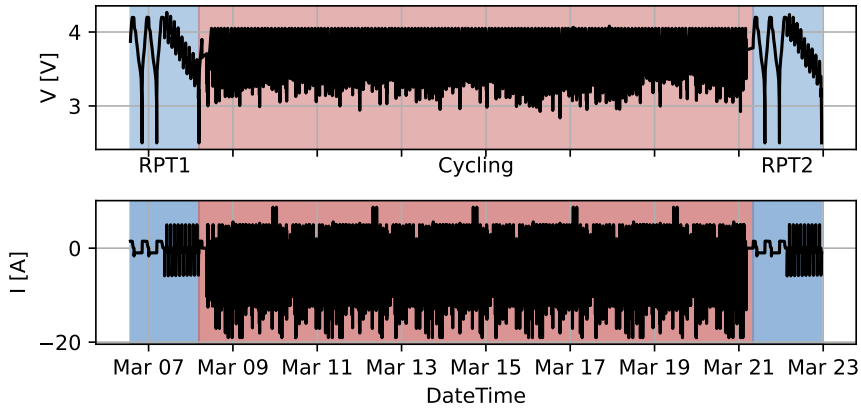

(a) Cycling period between two RPTs.

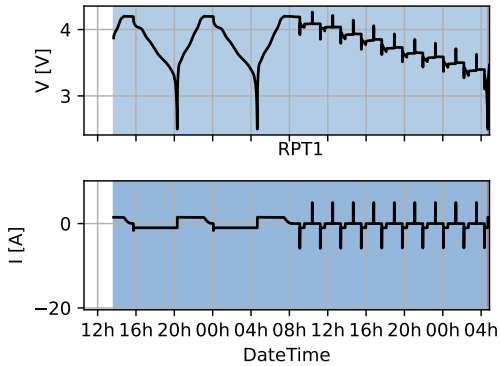

(b) Zoom-in view of a RPT.

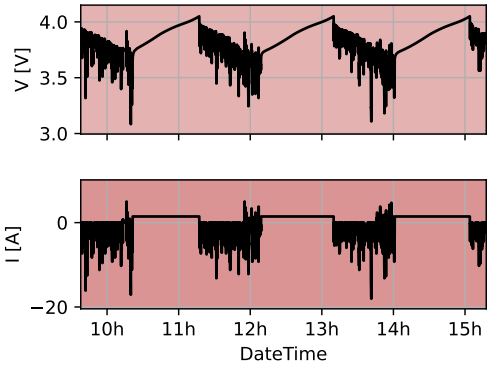

(c) Zoom-in view of a cycling test (driving + charge).

Figure 2: Representation of voltage and current during part of the testing.

Regarding the cycling tests, each of the cells tested aims to represent a driver who uses the EV to perform relatively homogeneous trips and charges after each use. Each driving cycle varies in duration, peak currents, resting times, etc. This aims to introduce variability common to real-world driving conditions, which is typically overlooked in standard cycling protocols consisting of constant test conditions (C-rate, DoD etc.). The synthetic cycles are obtained from a synthetic driving cycle model [8]. Figure 2c shows an example of a few synthetic driving cycles followed by a constant current charge at 0.5C.

The first cycling tests were performed at ambient temperature and later at 35ºC with the use of the climate chamber. For the purpose of this study it should be highlighted that the same charging rate was employed for the entire testing and that the ageing aims to represent cycling ageing conditions, with only short calendar ageing periods between some of the cycling tests and RPTs, which where not characterized.

After cycling and throughout the testing period, RPTs were performed to measure cell capacity and Internal Resistance (IR) at different SoC values. The capacity test consists of two sets of a full constant current - constant voltage charge at C/3 and a full discharge at 1C. An example of a RPT is shown in Figure 2b. The SoH is obtained considering the average between both discharges.

Figure 3 shows the evolution of the SoH over Full Equivalent Cycles (FEC) and time for each of the tested cells. Variability in the degradation rate is observed across the cells, reflecting differences in their cycling histories. Considering the last capacity measurement, the fastest degradation over FEC is observed for ALB2 followed by ALB5, ALB6, ALB1, ALB3 and ALB4.

2.2 Characterization methods

The characterization of battery operation during its first life relies on key variables such as voltage, current, temperature, and SoC. In this study, the analysis is conducted under laboratory conditions with constant temperature, thereby narrowing the scope to voltage, current and SoC profiles at the cell level. The focus is specifically placed on features related to driving periods that influence degradation. Charging phases, resting periods, and driving requirement characterization, essential for defining the SoF, are considered out of scope and will be addressed in future work.

The selected features are described below and visualized in Figure 4. Later a subindex 'V', 'Ich', 'Idis' or 'S' next to the feature will be used to refer to the voltage, charge current during regeneration, discharge current during driving or SoC profile, respectively.

- **Basic statistical features:** these features capture key aspects of the distribution and central tendency of the data. The mean (μ) provides the average value, the minimum (Min) and maximum (Max) represent the extreme values, the standard deviation (σ) measures the spread or variability, while skewness (γ_1) indicates the asymmetry of the data distribution, and the kurtosis (K) describes the sharpness of the peak of the distribution.

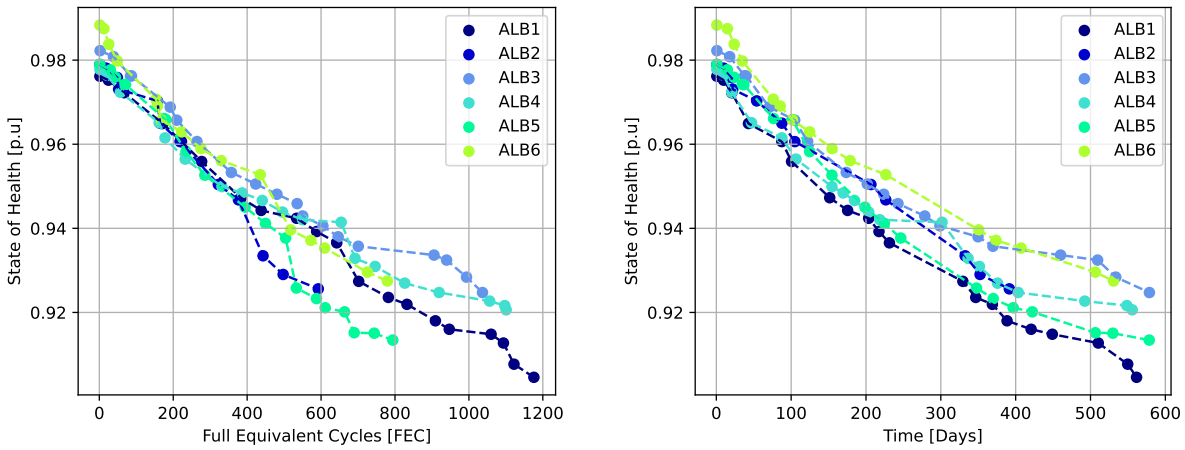

(a) Degradation over FECs.

(b) Degradation over time.

Figure 3: Evolution of the SoH for each of the cells.

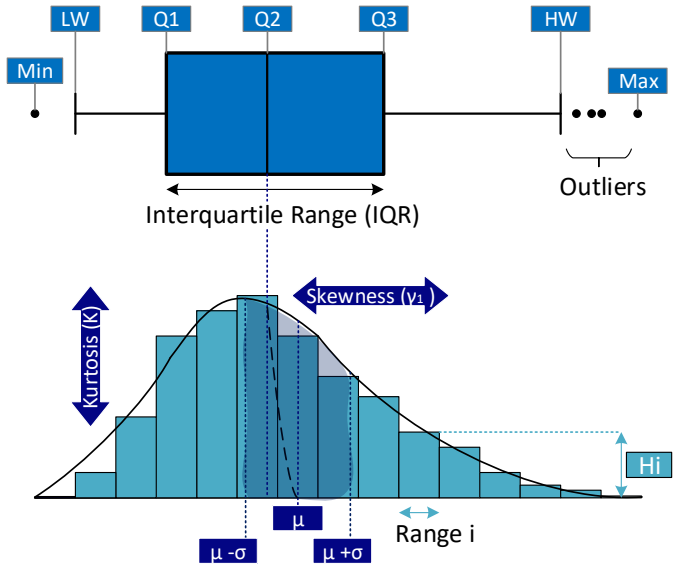

Figure 4: Graphical representation of characterization features.

- **Boxplot-based features:** a boxplot summarizes data by highlighting its spread and central tendency through quartiles. The first quartile ($Q1$) represents the 25th percentile, indicating that 25% of the data falls below this value. The median ($Q2$), or 50th percentile, divides the data in half, while the third quartile ($Q3$) marks the 75th percentile, meaning 75% of the data falls below this value. The whiskers extend from the quartiles to show the range of the data. The lower whisker (LW) represents the smallest value within 1.5 times the interquartile range (IQR) below Q_1, and the upper whisker (UW) represents the largest value within 1.5 times the IQR above $Q3$. Values outside of these whiskers are considered outliers.
- **Histogram-based features:** a histogram provides a visual representation of the data distribution by dividing the entire range of values into a set of bins. In this study, the ranges between the LW and the UW of the entire dataset (3 to 4.2 V for voltage, -14 to 0 for discharge current, 0 to 6.2 A for charge current, and 0-1 for SoC) are divided into five equally sized bins, following the square-root rule. The histogram-based features ($H1$-$H5$) represent the percentage of time that the battery spends in each interval.

2.3 Base degradation model

The objective of the base degradation model is to estimate the capacity fade (ΔSoH) between two RPTs based on operational data collected during the cycling period, as reflected by Figure 5. The degradation model incorporates a set of basic features that are known to significantly influence degradation. These include:

- ΔFEC: to capture differences in cycling lengths (in FEC).
- $\Delta Time$: to reflect differences in calendar periods (in days).
- FEC_0 *and* $Time_0$: initial values of FEC and time in days (to consider non-linearity of capacity fade over these variables)
- T_{cyc}: the average temperature during the cycling period in ºC.

The rest of the input features for the model represent the cycling conditions and depend on the characterization method employed (statistical, boxplot or histogram-based). Three models are built considering entire feature blocks for each characterization method. However due to the large number of features, a feature selection procedure is also applied.

Pearson and Spearman correlation coefficients are used as ranking criteria during feature selection to ensure that the most relevant features with respect to the target variable are retained for modeling. The

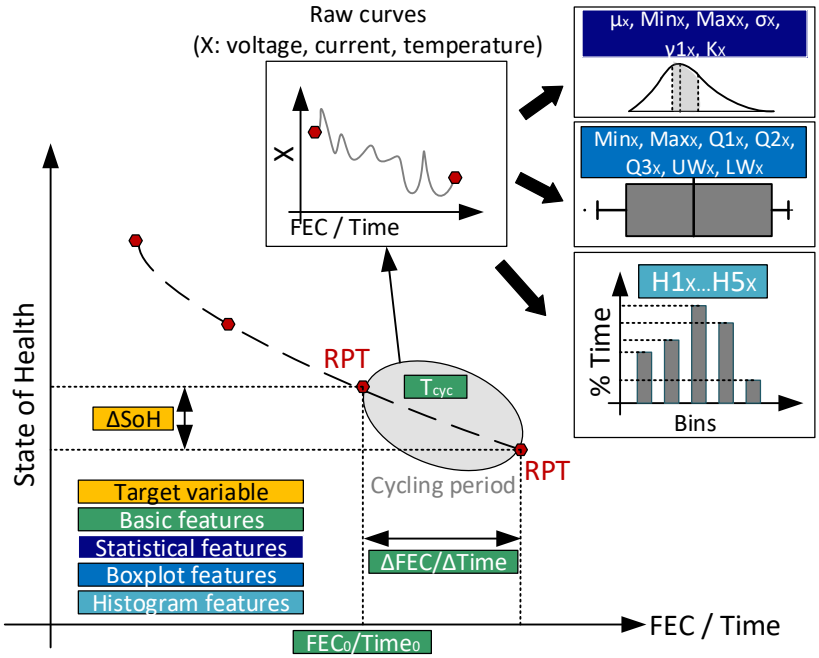

Figure 5: Graphical representation of the degradation model input/output.

Pearson correlation measures the strength of a linear relationship between each feature and the target, making it suitable for detecting proportional associations. In contrast, the Spearman correlation assesses the strength of a monotonic relationship, regardless of whether it is linear or not, by ranking the values and measuring correlation between the ranks.

The feature selection procedure first ranks the features by their absolute correlation (Pearson or Spearman) with the target variable (ΔSoH), then selects the top ten features. To reduce redundancy, pairwise correlations among the selected features are computed, and features with an inter-correlation above 0.75 are filtered out by discarding the ones with the lower correlation to the target. The resulting non-redundant feature subsets are used to train the models. Thus, 6 more models are built considering the two correlation coefficients and the 3 characterization methods.

Once the input features are defined, Gradient Boost Regression (GBR) is selected to build the base degradation model for this study due to its robustness and flexibility, particularly when working with small datasets. GBR is an ensemble learning method that builds a series of decision trees in a sequential manner, where each tree attempts to correct the errors of its predecessor. This iterative correction process makes GBR particularly well-suited for capturing complex relationships in the data, even when the available sample size is limited. Other regression models, such as linear regression, support vector machines, and random forests, were also tested, but generally underperformed GBR.

For each feature set, different combinations of hyperparameters are selected to find the most accurate one. In particular the number of estimators (N) tested are [10, 15, 20, 25], the maximum depth [3, 4, 5] and learning rates [0.1, 0.2, 0.25]. Among all models built, the one with the lowest Root Mean Square Error (RMSE) is selected as the tuned base model and is used as a reference for further comparison.

2.4 Data reduction methods

To minimize the amount of historical data that needs to be stored while maintaining acceptable model performance, different data reduction strategies were applied. The objective is to explore the tradeoff between data compression and the accuracy of the SoH predictions.

One approach is granularity reduction, which consists of decreasing the resolution of the original time series data. The baseline time series, recorded at 1-second intervals, was resampled to intervals of 3, 5, and 10 seconds. This reduction in data granularity significantly decreases the volume of stored informa-

tion. However, it may also lead to the loss of relevant high-frequency features, such as current or voltage spikes, which can be informative for degradation analysis.

A second strategy involves reducing data volume by characterizing each individual driving cycle using the same feature extraction methods applied to full time series. Instead of retaining raw data, only the resulting features per cycle are stored. To represent the entire period between two RPTs, these per-cycle features are aggregated. A weighted mean is applied to features where it makes sense to account for differences in driving cycle durations—giving more importance to longer cycles (e.g. μ or histogram-based features). However, not all features are suitable for weighted averaging: for some, such as minimum or maximum values, the global min/max is used, and for others, such as the boxplot quartiles, a simple arithmetic mean is applied.

To compare the different data reduction strategies two approaches can be considered:

- The first approach compares the accuracy of models retrained from scratch using the reduced datasets (3, 5, 10s granularity and aggregation). The goal of this approach is to evaluate whether 1s data is truly necessary during the model training stage in the laboratory, or if reduced datasets can be sufficient. For this, the same methodology used to train the baseline model is also applied to the new models. This includes the selection of features based on correlations, hyperparameter tuning, and other key steps in the model training pipeline. By applying this consistent methodology, the performance of models trained with reduced datasets can be fairly compared to the baseline model, ensuring that any observed differences in accuracy are due to the granularity changes rather than inconsistencies in the training process.
- The second approach is to assume that the existing degradation model has been built with the most descriptive data (1s granularity) but that the available data, where the predictions need to be made, has been reduced following the different strategys (3, 5, 10s granularity and aggregation). The goal of this comparison is to assesses how well a model trained on highly descriptive data generalizes and maintains accuracy when presented with less detailed data.

In both cases, the results are assesed from the perspective of the error increase (Eq. 1) and from the data compression ratio (Eq. 2).

$$\text{Error Difference } (\%) = \frac{\text{RMSE}_{\text{reduced}} - \text{RMSE}_{\text{baseline}}}{\text{RMSE}_{\text{baseline}}} \cdot 100 \tag{1}$$

$$\text{Compression Ratio} = \frac{\text{Data size}_{\text{reduced}}}{\text{Data size}_{\text{baseline}}} \tag{2}$$

3 Results

First, the results of the correlation analysis between the features and the target variable ΔSoH are shown. The features are grouped by variable (Voltage, charge current during regeneration Ich, discharge current Idis, and SoC) and the three characterization methods. A summary of the Pearson and Spearman correlation results are provided in Table 2 and 3, respectively.

Averaging across all signals, boxplot-based features tended to yield the highest mean correlation values, indicating that they effectively capture the underlying degradation signals. Histogram-based features

Table 2: Mean and Maximum Pearson correlation coefficients by variable and characterization method

Method	**Metric**	**Voltage**	**SoC**	**Ich**	**Idis**
All features	Mean	0.112	0.096	0.045	0.034
	Max	0.223 ($H4_V$)	0.189 (K_S)	0.095($Q1_{Ich}$)	0.051 ($Q3_{Idis}$)
Basic Statistics	Mean	0.097	0.112	0.037	0.032
	Max	0.223 (Max_V)	0.189 (K_S)	-0.063 (σ_{Ich})	-0.041 (σ_{Idis})
Boxplot	Mean	0.117	0.091	0.037	0.039
	Max	0.223 (Max_V)	0.140 (Max_S)	0.095 ($Q1_{Ich}$)	0.051 ($Q3_{Idis}$)
Histogram	Mean	0.145	0.083	0.055	0.031
	Max	0.223 ($H4_V$)	0.124 ($H3_S$)	-0.092 ($H4_{Ich}$)	-0.045 ($H4_{Idis}$)

Table 3: Mean and Maximum Spearman correlation coefficients by variable and characterization method

Method	**Metric**	**Voltage**	**SoC**	I_{ch}	I_{dis}
All features	Mean	0.107	0.059	0.072	0.038
	Max	0.228 (Max_V)	0.105 ($H1_S$)	0.140 (γ_{1Ich})	-0.120 (K_{Idis})
Basic Statistics	Mean	0.092	0.061	0.102	0.067
	Max	0.228 (Max_V)	-0.098 (γ_{1S})	0.140 (γ_{1Ich})	-0.120 (K_{Idis})
Boxplot	Mean	0.119	0.064	0.062	0.030
	Max	0.228 (Max_V)	0.089 (Min_S)	0.086 (Max_{Ich})	-0.064 ($Q3_{Idis}$)
Histogram	Mean	0.130	0.059	0.057	0.020
	Max	-0.181 ($H1_V$)	-0.105 ($H1_S$)	0.079 ($H1_{Ich}$)	-0.028 ($H4_{Idis}$)

followed closely, particularly for current signals, while basic statistical descriptors are generally less informative.

In general, features derived from voltage signals exhibit the highest levels of correlation, particularly when using histogram-based descriptors. SoC-related features also show moderate correlation, especially under boxplot and statistical methods. Current-based features, both for charge and discharge, tend to have lower correlation values across all characterization techniques. This indicates that voltage and SoC capture more relevant information for degradation trends compared to current-based features.

Table 4 summarizes the performance of the different models trained with various feature sets and selection strategies, ordered by increasing RMSE. Overall, using all available features tends to yield poorer results compared to selective approaches, likely due to redundancy and the inclusion of non-informative variables. Feature selection based on correlation, particularly using the Spearman method, improves model performance significantly. Among the characterization methods, boxplot-based features consistently achieve the lowest RMSE and highest R^2 values.

3.1 Tuned base model

Based on the results from Table 4, the model selected is the boxplot- and Spearman-based one. Figure 6 shows the correlation matrix among all features included in the model. As anticipated, the basic features initially considered, exhibit high correlations to the target, with the highest being ΔFEC and $\Delta Time$, followed by T_{cyc} and FEC_0. The only basic feature that is not included is $Time_0$ which showed excessively high correlation with FEC_0, indicating redundant information. Regarding the characterization features, the retained ones after the selection procedure are, in order of correlation, Max_V, UW_V, UW_{Ich}, Max_S, $Q3_{Idis}$ and $Q2_{Idis}$.

The scatter plot in Figure 7a visualizes the relationship between the ground truth values and the predicted ΔSoH values. Each point represents a single observation in the test dataset, with its x-coordinate indi-

Table 4: Model performance for different characterization and feature selection strategies, ordered by accuracy.

Characterization method	**Feature selection**	**N**	**Max depth**	**Learning rate**	**RMSE**	**R^2**
Boxplot-based	Based on Spearman	20	3	0.20	0.00132	0.759
Boxplot-based	Based on Pearson	20	4	0.25	0.00136	0.745
Basic statistical features	Based on Spearman	10	3	0.25	0.00142	0.721
Histogram-based	Based on Pearson	20	3	0.20	0.00148	0.697
Boxplot-based	All features	25	4	0.25	0.00159	0.650
Histogram-based	Based on Spearman	25	3	0.25	0.00158	0.653
Basic statistical features	Based on Pearson	25	3	0.20	0.00160	0.646
Basic statistical features	All features	20	3	0.25	0.00169	0.603
Histogram-based	All features	25	4	0.20	0.00184	0.532

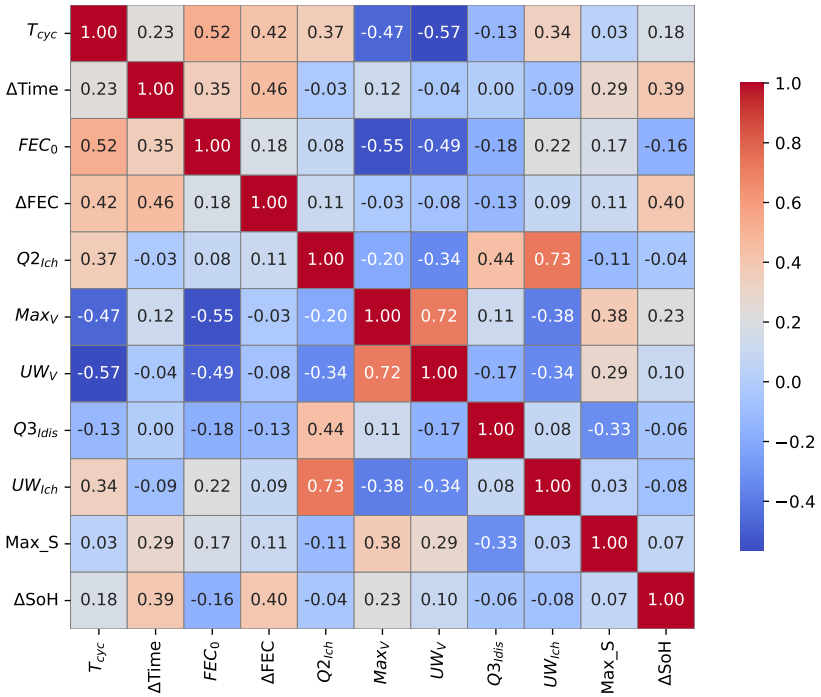

Figure 6: Spearman correlation matrix for the base model.

cating the actual value and its y-coordinate representing the corresponding prediction. A dashed red line representing the 45-degree line (where predicted values equal the ground truth) is included as a reference for ideal predictions. In this case, most points appear relatively close to the 45-degree line, suggesting a reasonable level of agreement between the predictions and the actual values, as also indicated by the model RMSE and R^2 values.

The density plot in Figure 7b indicates that the predicted values generally follow a similar distribution to the actual values, with the most frequent values occurring in the same range. This suggests that the degradation model captures the general distribution of the dataset. However, the degradation model underestimates the probability of observing degradation values in the higher range (above 0.010).

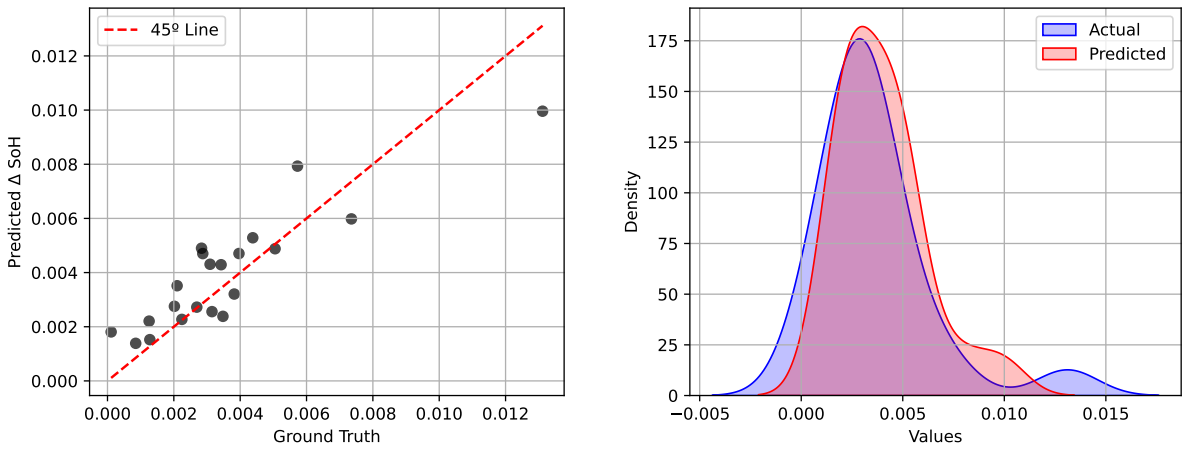

(a) Predictions of the model over ground truth.

(b) Density plots of the dataset and the predictions.

Figure 7: Results of the degradation base model.

3.2 Model accuracy versus data size trade-off

Table 5 presents the results of retraining the model using different downsampling strategies while keeping the same model training pipeline as the baseline. As the time granularity decreases, model performance generally declines, evident in lower R^2 values and higher errors. When the granularity is reduced to 3 seconds or lower, the error starts becoming more significant. This is because simple downsampling discards part of the signal's variability, resulting in the loss of important details that affect the model's accuracy.

The aggregated model, however, follows a different strategy. Instead of uniformly reducing the sample rate, it processes the full-resolution data (1s) within each driving cycle and extracts relevant features. This method preserves vital information, allowing the aggregated model to achieve performance similar to the baseline model while significantly reducing the dataset size. The error in the aggregated model is slightly higher because some features, particularly those based on boxplots or statistical metrics, cannot be aggregated in the same way. These features require access to the entire timeseries, and the error arises from the assumption made when averaging cycle-based features. The data compression for the aggregated case depends on the specific driving cycle duration, with the reported value representing the average for the employed dataset.

Table 5: Model performance comparison of different data reduction methods

Method	**Error difference**	**Data compression**
Baseline (1s granularity)	0%	1
3s granularity	+0.61%	1/3
5s granularity	+11.60%	1/5
10s granularity	+14.33%	1/10
Aggregated	+0.38%	∼1/1000

3.3 Model robustness to reduced data

Table 6 presents the results of the different data reduction methods but only when applied to the test dataset, meaning that the model employed in all cases is the base model using 1s data. It can be observed that there is a relevant error increase as the granularity decreases reaching close to a 20% error increase at 10s. The aggregation method also show a high error increase, making it an unsuitable approach to store real data when the available model is the one built with 1s timeseries.

However, the baseline model was trained using boxplot-based features. As mentioned, some of information required to obtain these features is lost when storing only cycle data instead of the entire timeseries. Instead, if histogram-based features are employed to build the base degradation model, the aggregated method would generate the same predictions as the baseline, since no information is lost when aggregating these features. Thus, considering the nature of histogram-based aggregation, which preserves the full distribution of the data without depending on the temporal resolution, this approach stands out as a highly efficient solution to reduce data size while maintaining high predictive accuracy.

Table 6: Prediction accuracy when reducing test dataset

Method	**Error difference**	**Data compression**
Baseline (1s granularity)	0%	1
3s granularity	+7.58%	1/3
5s granularity	+9.11%	1/5
10s granularity	+19.30%	1/10
Aggregated	+21.25%	∼1/1000

4 Discussion

Compared to most existing degradation models, which typically rely on static laboratory-generated datasets with fixed cycling conditions, the methods proposed in this work are designed to better accom-

modate the variability inherent in real-world driving profiles. Recent studies have begun to recognize the need for models that can generalize beyond constant operating conditions, reflecting the diverse usage patterns encountered in electric vehicles [9, 10]. In addition, a significant contribution of this study has been dedicated to minimizing the amount of data that must be stored while preserving model accuracy. This aspect is increasingly critical, both from an economic perspective, due to the growing scale of battery testing and monitoring, and from an environmental standpoint, aligning with the interest in reducing the digital carbon footprint associated with large-scale data management.

Considering the broader context of battery circularity, the outcomes of this research offer several key contributions. By identifying the most informative features for assessing battery health and predicting degradation, this work provides essential data points that can be incorporated into a Battery Passport. This standardized record of a battery's history and condition is crucial for facilitating informed decisions regarding second-life applications, remanufacturing, and recycling. Accurate degradation models, built upon the characterized driving profiles, help estimate the RUL of a battery, enabling its transition into second-life applications and the development of innovative concepts such as dynamic warranties. This optimized lifespan management directly supports the principles of a circular economy by maximizing the value and minimizing the waste associated with EV batteries.

Despite the valuable insights gained, the dataset utilized in this study presents certain limitations. The absence of data encompassing calendar aging periods and the maintenance of a constant temperature throughout the experiments restrict the scope of the findings to cycle-related degradation under specific conditions. Furthermore, the analysis focuses on six distinct use cases, and the results obtained may vary for different battery cell chemistries and formats.

Thus, different possibilities for future research emerge from this study. Expanding the analysis to encompass larger and more diverse datasets, including data with varying cell chemistries, temperatures and calendar aging effects, can help reach a more comprehensive understanding of battery degradation under real-world conditions. Furthermore, exploring the efficacy of different machine learning models beyond those employed in this study could potentially lead to even more accurate degradation predictions. Finally, since this work has focused on characterizing degradation related factors, an important direction for future work lies in developing robust characterization methods specifically tailored for the prediction of SoF, a critical parameter for evaluating a battery's ability to perform its intended tasks over time.

5 Conclusions

This work proposes and evaluates different methods to characterize driving cycles for battery degradation modeling in order to reduce the amount of data required for SoH prediction. Among the various signals analyzed, voltage and SoC appear as the most sensitive to degradation, consistently showing stronger correlations with capacity fade compared to current-based features.

Boxplot-based modeling, coupled with feature selection methods, provides the best overall performance, achieving the lowest prediction errors when estimating degradation from driving cycle data. In addition to model accuracy, the impact of data resolution is explored by reducing the granularity of the timeseries or storing only aggregated information per driving cycle. Results show that when models are trained aggregating the features per cycle the model is as accurate as when training with the entire timeseries at 1s granularity, offering a viable alternative for efficient data storage without sacrificing prediction quality.

Model robustness to reduced data is further assessed by applying the base model trained on 1s timeseries to test datasets of lower resolution. In this case, a notable loss of accuracy is observed, particularly when simple downsampling is applied. However, the use of aggregated data once again emerges as the most reliable approach to preserve model performance, provided that histogram-based features are used. Histogram-based modeling not only maintains predictive accuracy under data reduction but also offers an intuitive interpretation of cycle behavior, making it an attractive strategy for practical implementation.

This work provides insights for several practical applications. The proposed characterization methods can contribute to the development of more accurate degradation models, particularly under dynamic operating conditions. Additionally, the ability to reduce the volume of laboratory testing data without compromising prediction accuracy supports more efficient data storage and management practices. Finally, by facilitating compact yet informative data representations, this approach can enhance the implementation of initiatives such as dynamic warranties and provide inputs for the Battery Passport.

Acknowledgments

This study has received funding from the European Union's Horizon 2020 research and innovation program under grant agreement No. 963580 (ALBATROSS project). This funding includes funds to sup-

port research work and open access publications. The work has also been supported by the project Netbuild (CPP2021-009031) and by the assistance of the RYC2021-033477-I grant both funded by MCIN/AEI/10.13039/501100011033 and by the European Union – NextGenerationEU/PRTR.

References

[1] J. L. Richter, "A circular economy approach is needed for electric vehicles," *Nature Electronics*, vol. 5, no. 1, pp. 5–7, Jan. 2022. [Online]. Available: https://www.nature.com/articles/s41928-021-00711-9

[2] "Regulation (EU) 2023/ of the European Parliament and of the Council of 12 July 2023 concerning batteries and waste batteries, amending Directive 2008/98/EC and Regulation (EU) 2019/1020 and repealing Directive 2006/66/EC."

[3] T. Montes, M. Etxandi-Santolaya, J. Eichman, V. J. Ferreira, L. Trilla, and C. Corchero, "Procedure for Assessing the Suitability of Battery Second Life Applications after EV First Life," *Batteries*, vol. 8, no. 9, p. 122, Sep. 2022. [Online]. Available: https://www.mdpi.com/2313-0105/8/9/122

[4] M. Etxandi-Santolaya, T. Montes, L. C. Casals, C. Corchero, and J. Eichman, "Data-Driven State of Health and Functionality Estimation for Electric Vehicle Batteries Based on Partial Charge Health Indicators," *IEEE Transactions on Vehicular Technology*, pp. 1–15, 2024. [Online]. Available: https://ieeexplore.ieee.org/document/10766661/

[5] M. Lucu, E. Martinez-Laserna, I. Gandiaga, K. Liu, H. Camblong, W. Widanage, and J. Marco, "Data-driven nonparametric Li-ion battery ageing model aiming at learning from real operation data - Part B: Cycling operation," *Journal of Energy Storage*, vol. 30, p. 101410, Aug. 2020.

[6] J. Olmos, I. Gandiaga, A. Saez-de Ibarra, X. Larrea, T. Nieva, and I. Aizpuru, "Modelling the cycling degradation of Li-ion batteries: Chemistry influenced stress factors," *Journal of Energy Storage*, vol. 40, p. 102765, Aug. 2021.

[7] Albatross, "Albatross H2020 EU." [Online]. Available: https://albatross-h2020.eu

[8] M. Etxandi-Santolaya, L. Canals Casals, and C. Corchero, "Estimation of electric vehicle battery capacity requirements based on synthetic cycles," *Transportation Research Part D: Transport and Environment*, vol. 114, p. 103545, Jan. 2023.

[9] F. von Bülow and T. Meisen, "A review on methods for state of health forecasting of lithium-ion batteries applicable in real-world operational conditions," *Journal of Energy Storage*, vol. 57, p. 105978, Jan. 2023. [Online]. Available: https://linkinghub.elsevier.com/retrieve/pii/S2352152X22019661

[10] R. R. Richardson, M. A. Osborne, and D. A. Howey, "Battery health prediction under generalized conditions using a Gaussian process transition model," *Journal of Energy Storage*, vol. 23, pp. 320–328, Jun. 2019.

Presenter Biography

Maite Etxandi Santolaya is an Industrial Engineer from the University of the Basque Country. She holds a double Master's degree in Industrial Engineering and Energy Engineering from the Polytechnic University of Catalonia (UPC). She obtained her PhD in the Environmental Engineering Program from UPC, which aimed to improve battery End of Life estimation to maximize their use and reduce their environmental impact. Currently, she works at the Catalonia Institute for Energy Research (IREC) in the Energy Systems Integration group, focusing on modeling and state estimation for electric vehicle batteries.